05.2;12.1;13.2

Violation of the conformity between the induction current and the emission current during the pyroelectric effect in a single crystal of lithium tantalate under vacuum conditions

© A.N. Oleinik[1], M.E. Gilts[1], P.V. Karataev[2], A.A. Klenin[1], A.S. Kubankin[1,3], P.G. Shapovalov[4]

[1] Laboratory of Radiation Physics, Belgorod State National Research University, Belgorod, Russia
[2] John Adams Institute at Royal Holloway, University of London, Egham, U.K.
[3] Lebedev Physical Institute, Russian Academy of Sciences, Moscow, Russia
[4] National Research Nuclear University „MEPhI", Moscow, Russia
E-mail: oleynik_a@bsu.edu.ru

Received January 30, 2023
Revised February 21, 2023
Accepted March 10, 2023

A comparison of the induction current and the emission current during the pyroelectric effect under vacuum conditions with periodic variation in the temperature of a single crystal of lithium tantalate is presented. An increase in the variation frequency leads to suppression of the emission current, which prevents observing the effect of the optimal frequency with the maximum amplitude as in the case of the induction current. The conformity of both current forms is shown, except for the region of 2 mHz and less where an additional current wave is observed. It is established that this additional wave is initiated above a certain threshold of potential difference and leads to its stabilization.

Keywords: pyroelectric effect, ferroelectric electron emission, pyroelectric accelerator, lithium tantalate.

DOI: 10.21883/TPL.2023.05.56023.19514

Ferroelectric electron emission is distinguished from the field electron emission due to unique emitting-flux properties which stem from peculiar features of the structure of ferroelectric materials [1]. It is possible to distinguish two subtypes of the ferroelectric electron emission: the „strong" and „weak" ones. In the case of the „strong" emission, pulsed electron fluxes of up to a few amperes can be created by applying electric field to the electrodes covering the polar surfaces of the material [2]. The „weak" electron emission allows obtaining only much lower values of current, namely, of about $1-10$ nA, however, the emission process itself is of the long-term continuous character [3]. In this case, the emission proceeds because of variations in the material temperature leading to the charge induction onto the material polar surfaces due to the pyroelectric effect. The outstanding properties of this mode are self-focusing and monochromaticity of the electron flux up to the energy of 200 keV [4].

Based on the ratio between the induction and emission currents during the pyroelectric effect, it is possible to estimate the efficiency of the „weak" electron emission that is applicable in pyroelectric accelerators [5]. In our recent work we showed that, when the temperature is varied periodically according to the sinusoidal law, there exists a certain frequency range where the induction current amplitude is maximal [6]. This fact stimulated our further research aimed at revealing the ratio between the induction and emission currents under periodic temperature variations versus the variation frequency.

Fig. 1 presents the schemes for measuring the induction and emission currents. Each scheme is based on the assembly consisting of the heat sink *1*, Peltier element *2*, and lithium tantalate ($LiTaO_3$) single crystal *3*. Using a signal generator, the Peltier element was supplied with a signal with the preset frequency and power, which induced sinusoidal temperature variation [7] in the range from 15 to 40°C. The current was measured with picoammeter Keithley 6485. The measurements were performed by using a z-oriented cylindrical single crystal 20 mm in diameter and 10 mm in height (produced at the Kola Center of RAS, Apatity). In measuring the induction current, two aluminum-foil electrodes were secured with conductive epoxy glue on the $LiTaO_3$ polar surfaces. When the emission current was measured, the top surface remained free, and the top electrode was located at the distance of 10 mm from it. In order to prevent the current loss in air, as well as the effect of impact ionization, the residual gas pressure during measuring the emission current was kept at the level of 1 mTorr. In both cases, the circuit was represented by connected in series picoammeter and capacitor whose insulator consists, in one case, of a single crystal, and, in another case, of a single crystal and vacuum gap.

Fig. 2 demonstrates the case curves of the induction and emission currents at the frequencies of 2 and 8 mHz. One can observe the identity of the shapes of both curves; however, this identity is violated at 2 mHz. The emission current curve exhibits an additional current wave commencing after passing the peak value at about $\pi/2$. The

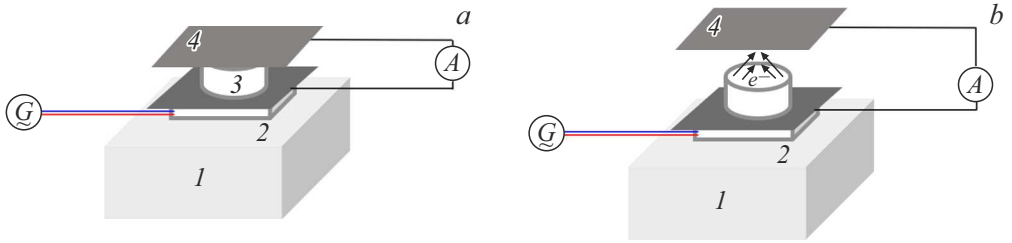

Figure 1. Measurement schemes for the induction (a) and emission (b) currents. *1* — heat sink, *2* — Peltier element and bottom electrode, *3* — single-crystal lithium tantalate, *4* — top electrode.

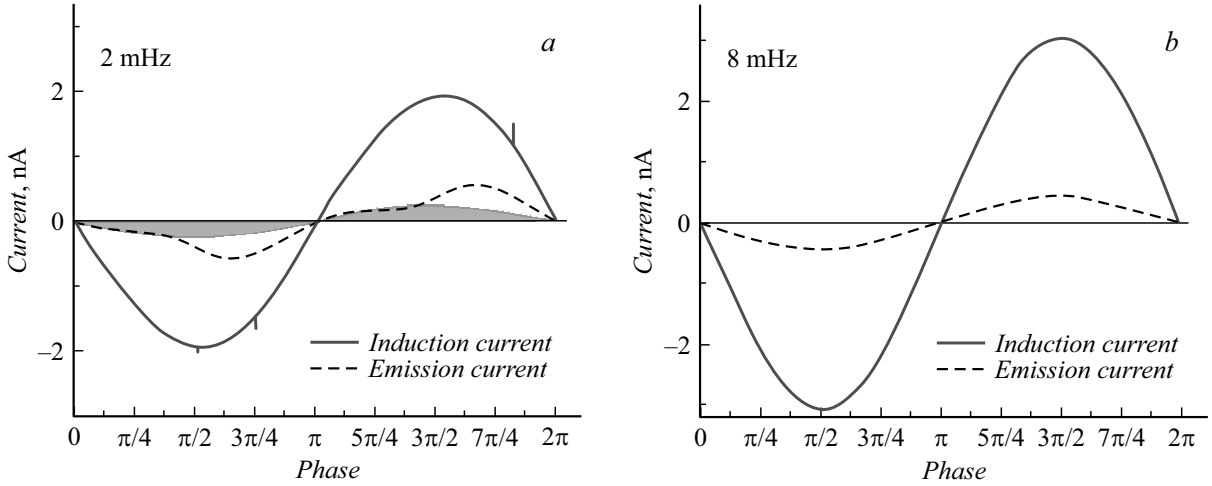

Figure 2. Curves of the induction and emission currents under periodic variations in the $LiTaO_3$ temperature with the frequencies of 2 (a) and 8 mHz (b). In the case of 2 mHz, the emission current component corresponding to the expected current is colored gray.

additional wave has a peak at about $3\pi/4$ and terminates by the moment of the current polarity inversion.

Notice that the emission current amplitude increases with increasing frequency much weaker than the induction current amplitude; therefore, in the case of the emission current, the effect of the existence of a frequency band where the current amplitude is maximal [6] is much less pronounced. Fig. 3, *a* presents a diagram of ratios between the integrals of the induction current, emission current and additional wave current in the frequency range of 0.5–8 mHz. As frequency increases, all the integrals decrease due to the decrease in the temperature oscillation amplitude. Notice that the ratio of the emission current integral to the induction current integral decreases much faster. This fact may be interpreted as an evidence of the fact that the emission current depends on the amount of charge accumulated on the pyroelectric surface. A lower amount of charge promotes a lower electric field strength and a higher potential barrier to the electron emission. Notice that the additional current wave is observed at the frequencies of up to 2 mHz, and its contribution decreases with increasing frequency even faster.

The induction current integral with subtracted emission current integral may be assumed to represent the amount of charge on the single-crystal surface, which creates the electric field. Using the computer modeling, it is possible to estimate the potential difference taking into account the peculiarities of the charge distribution over the crystal surface [8]. On the other hand, the potential difference may be estimated experimentally through the X-ray radiation cutoff energy [9]. Fig. 3, *b* illustrates the comparison of the simulated and experimentally obtained estimates of the half-cycle potential difference at 1 and 6 mHz. The presented direct experimental estimate was obtained by measuring the X-ray spectrum concurrently with the emission current in the experimental geometry shown in [10]. The model estimation of the potential difference was performed by simulating the experiment in the COMSOL Multiphysics code with presetting the total amount of charge on the single-crystal surface according to the following formula:

$$Q_{sum}^{n} = \sum_{j=1}^{n} \left(i_{pyr} - i_{em}\right)_j, \qquad (1)$$

where Q_{sum}^{n} is the total amount of charge at the n-th time moment, i_{pyr} is the induction current, i_{em} is the emission current.

At the frequency of 6 mHz, a good agreement between the experimental and model estimates is observed, which evidences for insignificant leakage currents. At the same time, at 1 mHz there takes place a very large discrepancy between those two estimates; this, on the one hand, may

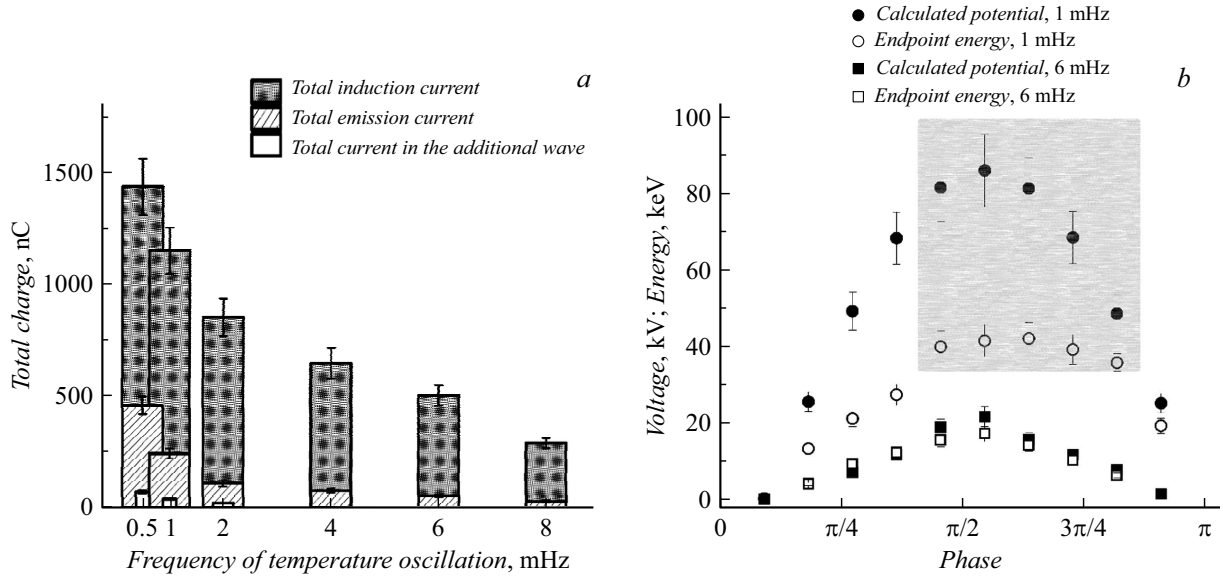

Figure 3. *a* — ratios between integrals of the induction current, emission current and additional wave current. *b* — variation in the calculated difference of potentials (filled symbols) and X-ray cutoff energy (empty symbols) at the frequency of 1 mHz (circles) and 6 mHz (squares). The shaded area indicates the range where the additional wave is observed.

be associated with an increase in the leakage current [11] and, on the other hand, with the observed emission-current additional wave. This area is highlighted in Fig. 3, *b*; here are observed deviations from the wave-like shape of the potential difference variation and its saturation at approximately the same value. The difference of potentials at which the additional wave commences is approximately the same in all the measurements in the given experimental geometry and is somewhat higher than 30 kV.

Thus, the observed additional wave of the emission current violates the conformity between the emission current and induction current and is initiated only when a certain potential difference is reached, which restricts its increase and causes its stabilization. Under the experimental conditions, the increase in the oscillation frequency leads to a decrease in the generated potential difference, which suppresses the effect of the emission-current additional wave and makes absolutely identical the shapes of the induction and emission currents. Along with this, the effect of electron emission itself also gets suppressed with increasing oscillation frequency. This makes it possible to conclude that the effect of the optimal frequency of the pyroelectric material temperature variation [6] can hardly be applied in generating strong electric fields and initiating more efficient electron emission.

Financial support

The study was supported by the Russian Science Foundation (project № 21-72-00006). The work of A.S. Kubankin and P.G. Shapovalov devoted to designing the experimental bench was financially supported a Program of the Ministry of Education and Science of the Russian Federation for higher education establishments, Project No. FZWG-2020-0032 (2019-1569).

Conflict of interests

The authors declare that they have no conflict of interests.

References

[1] G. Rosenman, D. Shur, Ya. Krasik, A. Dunaevsky, J. Appl. Phys., **88**, 6109 (2000). DOI: 10.1063/1.1319378
[2] H. Gundel, H. Riege, J. Handerek, K. Zioutas, Appl. Phys. Lett., **54**, 2071 (1989). DOI: 10.1063/1.101169
[3] J.D. Brownridge, *Trends in electro-optics research* (Nova Science Publ., N.Y., 2005).
[4] J.D. Brownridge, S.M. Shafroth, Appl. Phys. Lett., **79**, 3364 (2001). DOI: 10.1063/1.1418458
[5] N. Kukhtarev, T. Kukhtareva, M. Bayssie, J. Wang, J.D. Brownridge, J. Appl. Phys., **96**, 6794 (2004). DOI: 10.1063/1.1808479
[6] A. Oleinik, M. Gilts, P. Karataev, A. Klenin, A. Kubankin, J. Appl. Phys., **132**, 204101 (2022). DOI: 10.1063/5.0124599
[7] L.E. Garn, E.J. Sharp, J. Appl. Phys., **53**, 8974 (1982). DOI: 10.1063/1.330454
[8] R. Ghaderi, F.A. Davani, Appl. Phys. Lett., **105**, 232906 (2014). DOI: 10.1063/1.4903891
[9] A.N. Oleinik, E.V. Bolotov, M.E. Gilts, O.O. Ivashchuk, A.A. Klenin, A.S. Kubankin, A.V. Shchagin, Bull. Lebedev Phys. Inst., **48**, 127 (2021). DOI: 10.3103/S1068335621050079.
[10] P. Karataev, A. Oleinik, K. Fedorov, A. Klenin, A. Kubankin, A. Shchagin, Appl. Phys. Exp., **15**, 066001 (2022). DOI: 10.35848/1882-0786/ac6b82
[11] A.N. Oleinik, P.V. Karataev, A.A. Klenin, A.S. Kubankin, K.V. Fedorov, A.V. Shchagin, Russ. Phys. J., **63**, 119 (2020). DOI: 10.1007/s11182-020-02010-w.

Translated by Solonitsyna Anna